

Reconciling Fractional Power Potential and EGB Gravity in the light of ACT

Mehnaz Zahoor^{ID*}

Department of Physics, Central University of Kashmir, Ganderbal J&K- 191131

Suhail Khan^{ID†}

Centre for Theoretical Physics, Jamia Millia Islamia, New Delhi 110025, India

Imtiyaz Ahmad Bhat^{ID‡}

Department of Physics, Islamic University of Science and Technology, Awantipora, J&K- 192122

Recent results from the ACT collaboration indicate a higher value for the scalar spectral index, with $n_s = 0.9743 \pm 0.0034$, which sets the tighter constraints on inflationary models and these shifts are not in favor of many pre-existing scenarios, including the widely studied and accepted standard Starobinsky model. In this paper we examine the fractional power scalar potential within the framework of Einstein–Gauss–Bonnet (EGB) gravity incorporating standard slow-roll approximation. The EGB theory, motivated by higher-dimensional models, introduces quadratic curvature corrections and a coupling between the scalar field and the Gauss–Bonnet term, thereby modifying the cosmological dynamics. The results show good agreement with observational data, placing the predictions within the 1σ region of the ACT r – n_s constraint plot. Furthermore, incorporating the running of the scalar spectral index reinforces the model's consistency with observational bounds. We also explore the parameter space of the EGB couplings and identify the range of free parameters for which the results of n_s and r values remain within the 1σ region of the ACT constraints. Finally, we also investigate the reheating phase, demonstrating that the model not only agrees with ACT data but also satisfies the lower bound on the reheating temperature, thereby ensuring a consistent and viable cosmological scenario.

I. INTRODUCTION

Although the inflation in the early Universe resolves many problems like horizon, flatness, and monopole problems, it anticipates quantum fluctuations that serves as the seed for the universe's large-scale structure formation [1–9]. The data from observations [10–12] collected over the past few decades strongly substantiated the model of inflation and is now the fundamental component of all cosmological models. Since the first proposal of inflationary cosmology, the model has been developed in different ways [13–37]. The model has been thoroughly investigated in different scenarios and in numerous modified gravity theories [38]. The inflationary phase is driven by a scalar field slowly rolling down a flat potential towards its minimum, which in return fuels a quasi-de Sitter expansion, leading to a rapid expansion of the universe's size over a short epoch of time.

Recent data from the Atacama Cosmology Telescope (ACT) shows that the scalar spectral index n_s is on higher side as compared to what *Planck* observations reported earlier. After a combined look at *Planck* and ACT data, the scalar spectral index is measured as $n_s = 0.9709 \pm 0.0038$. By incorporating further information from CMB, BAO, and DESI, the value rises to $n_s = 0.9743 \pm 0.0034$ [39, 40].

This new observational discovery suggests that several widely accepted inflationary models, including the Starobinsky model [7], which was compatible with the earlier data, are now disfavored since they stand on the 2σ border. This shift in the r – n_s parameter space highlights how crucial it is to update and improve the consistent infla-

tionary models. Consequently, in light of the most recent observational evidence, the wide class of inflationary models need to be revisited[41–78].

A reheating phase is necessary to re-populate the Universe, which is in a cold condition at the end of inflation[79]. Standard particles are produced during the reheating phase by the decay of the scalar field. Interactions between the produced particles cause the universe to warm, facilitating a seamless transition to the radiation phase (for a more thorough description of the reheating, see [80, 81]). Any observation does not strictly constrain the reheating temperature.

However the BBN provides a lower range for the reheating temperature, $T_{BBN} \simeq 10^{-2}$ GeV, while as the scale at which inflation occurs provides an upper limit, $T_{re} < 10^{16}$ GeV. The reheating temperature thus has a broad valid available range from inflation to BBN.

One can get low values of the tensor-to-scalar ratio, r [82, 83], in cosmological models, having a non-minimal coupling. But the recent observations allow a relatively small upper bound on the tensor-to-scalar ratio, $r < 0.038$ (P-ACT-LB-BK18), which has drawn attention to these models. However, superstring theory-inspired gravitational theories with higher-order curvature terms conclude that, in addition to the higher-order curvature terms, there should be a non-minimal interaction between the scalar field and the geometry. Thus, there is a compelling need to take into account modified gravity theories in order to comprehend the early stages of evolution of our Universe. Even the inflation potentials that are not allowed in Einstein gravity can be reconciled by modified gravity theories [84–101].

Here, we are interested in investigating the fractional power Potential in the framework of EGB gravity, which is a modified gravity theory that incorporates quadratic curvature corrections and is determined by the higher-

* mehnazzahoormir@gmail.com

† suhail@ctp-jamia.res.in

‡ bhat.imtiyaz@iust.ac.in

dimensional theory. A scalar field with a non-minimal coupling to the GB component is present in the theory and is described by $\xi(\phi)$ [102–135]. The dynamics of the universe is mainly influenced by the Gauss-Bonnet term. In string theory, it functions as a quantum correction to the Einstein-Hilbert action. Here, we look into inflation in the EGB gravity frame using two well-motivated GB coupling functions one as hyperbolic [136–138] and other as exponential [139–142] and the form of these couplings is given implicitly in Eq. 11. It is believed that the fractional potential describes the potential of the scalar field. We find that the model shows high agreement with the ACT data, and the anticipated values of the scalar spectral index and the tensor-to-scalar ratio remain within the 1σ area, despite the potential being disfavored in the Eisenstein gravity. We also take into account the reheating phase, as well as how the reheating temperature and e-fold behave in relation to the scalar spectral index. We find that for $\omega_{re} > 1/3$, the model can both meet the reheating temperature requirement and achieve high agreement in 1σ range for different sets of model parameters in concordance with the ACT data.

Our analysis is structured as follows: we provide a quick overview of the EGB gravity theory in Sec.II. Next, we apply the slow-roll approximations to redefine the key dynamical equations and explore the inflationary and reheating phases in Sec.III. The ACT data is compared with the model's output from the slow-roll approach in Sec.IV for hyperbolic coupling and in Sec.V for exponential coupling respectively. Lastly, we provide a summary of our analysis in Sec.VI.

II. EGB BACKGROUND

The action of the model is given by [109]

$$S = \int d^4x \sqrt{-g} \left[\frac{R}{2} - \frac{1}{2} g^{\mu\nu} \partial_\mu \phi \partial_\nu \phi - V(\phi) - \frac{1}{2} \xi(\phi) \mathcal{G} \right], \quad (1)$$

where

$$\mathcal{G} = R_{\mu\nu\rho\sigma} R^{\mu\nu\rho\sigma} - 4R_{\mu\nu} R^{\mu\nu} + R^2,$$

is the quadratic curvature correction term also known as GB term, g is the determinant of the metric $g_{\mu\nu}$, $R, R_{\mu\nu}, R_{\mu\nu\rho\sigma}$ is the Ricci scalar, Ricci tensor, Riemann tensor of corresponding metric $g_{\mu\nu}$ respectively, and $V(\phi)$ is the potential of the scalar field ϕ .

Assuming homogeneity and isotropy, the large-scale geometry of the universe is described by a spatially flat FLRW metric. Under this assumption, the modified Friedmann equations can be derived accordingly.

$$6H^2 \left(1 - 4\xi_{,\phi} \dot{\phi} H \right) = \dot{\phi}^2 + 2V, \quad (2)$$

$$2\dot{H} \left(1 - 4\xi_{,\phi} \dot{\phi} H \right) = -\dot{\phi}^2 + 4H^2 \Psi, \quad (3)$$

and for the dynamics scalar field, the equation is written as

$$\ddot{\phi} + 3H\dot{\phi} = -V_{,\phi} - 12H^2 \xi_{,\phi} \left(\dot{H} + H^2 \right), \quad (4)$$

Here, Ψ is defined as

$$\Psi = \xi_{,\phi\phi} \dot{\phi}^2 + \xi_{,\phi} \ddot{\phi} - H \xi_{,\phi} \dot{\phi},$$

where $H = \dot{a}/a$ is the Hubble parameter, and *dot* denotes a derivative with respect to cosmic time. In case of a varying coupling function, i.e., $\xi_{,\phi} \neq 0$, Eqs. (3) and (4) do not represent the full dynamical system. The correct dynamical equation can be derived from Eqs. (2) and (4) and performing algebraic transformations; for further details, see Ref. [143].

$$\begin{aligned} \frac{d\phi}{dN} &= \chi, \\ \frac{d\chi}{dN} &= \frac{1}{H^2(B - 2\xi_{,\phi} H^2 \chi)} \left(3[3 - 4\xi_{,\phi\phi} H^2] \xi_{,\phi} H^4 \chi^2 + [3B + 2\xi_{,\phi} V_{,\phi} - 3] H^2 \chi - 4V^2 X \right) - \frac{\chi}{2H^2} \frac{dH^2}{dN}, \\ \frac{dH^2}{dN} &= \frac{H^2}{2(B - 2\xi_{,\phi} H^2 \chi)} \left((4\xi_{,\phi\phi} H^2 - 1) \chi^2 - 16\xi_{,\phi} H^2 \chi - 16V^2 \xi_{,\phi} X \right). \end{aligned} \quad (5)$$

Here, χ is defined as $\chi = \dot{\phi}/H$, and a change of variables has been applied to express the equations in terms of the number of e-folds, $N = \ln(a/a_e)$, rather than cosmic time t , using the relation $dN = H dt$. The quantities B and X are defined as follows:

$$B = 12\xi_{,\phi}^2 H^4 + \frac{1}{2}, \quad X = \frac{1}{4V^2} (12\xi_{,\phi} H^4 + V_{,\phi}). \quad (6)$$

The dynamics of the inflationary phase are characterized

by the slow-roll parameters, which are defined as:

$$\varepsilon_1 = -\frac{\dot{H}}{H^2} = -\frac{d \ln(H)}{dN}, \quad \varepsilon_{i+1} = \frac{d \ln |\varepsilon_i|}{dN}, \quad i \geq 1, \quad (7)$$

In EGB gravity, there are additional slow-roll parameters in addition to the above-mentioned parameters in Eq.(7). These parameters are however, associated with the coupling

term, and are defined as:

$$\delta_1 = 4\xi_{,\phi}H^2\chi, \quad \delta_{i+1} = \frac{d\ln|\delta_i|}{dN}, \quad i \geq 1. \quad (8)$$

In terms of these slow-roll parameters, the evolution equations get redefined as discussed in Ref. [143]. Consequently, both the scalar spectral index and the tensor-to-scalar ratio can also be expressed in terms of these slow-roll parameters which are now dependent on coupling term and are given as:

$$n_s = 1 - 2\varepsilon_1 - \frac{2\varepsilon_1\varepsilon_2 - \delta_1\delta_2}{2\varepsilon_1 - \delta_1}, \quad r = 8|2\varepsilon_1 - \delta_1|. \quad (9)$$

III. INFLATION AND SUBSEQUENT REHEATING PHASES

This section considers the inflationary and reheating phases within the EBG background. The potential under consideration is fractional power law originally proposed by [144], though disfavored in the context of standard gravity, but can be rescued in EGB when confronted with recent ACT data.

$$V(\phi) = V_0 \phi^n \quad (10)$$

where the power index n is set to $(1/3, 2/5, 2/3, 4/3)$. The choice of n values is motivated from different literature surveys and observational data. The choice for $n = 2/3$ and $4/3$ are considered in the context of the *Planck* results, $n = 1/3$, $2/5$ and $2/3$ are inspired from Ref.[145] and $n = 1/3$, $2/3$ are further supported from ACT DR6 constraints on extended cosmological models.

Two commonly used forms of the Gauss–Bonnet (GB) coupling function are considered [99, 106, 112, 134, 135, 139–142] and defined as follows:

$$\xi(\phi) = \frac{\xi_1}{V_0} \tanh(\xi_2 \phi), \quad \xi(\phi) = \frac{\xi_1}{V_0} e^{-\xi_2 \phi} \quad (11)$$

Here, ξ_1 and ξ_2 are free coupling parameters. The constant V_0 is introduced to simplify subsequent calculations and does not affect the generality of the analysis, because most of the slow roll parameters are independent of V_0 . This work follows the effective potential method developed in [109, 146, 147], where the stability of de Sitter solutions in the model has been investigated. The effective potential is expressed in terms of the scalar field potential and the coupling function as follows:

$$V_{eff}(\phi) = -\frac{1}{4V(\phi)} + \frac{1}{3}\xi(\phi). \quad (12)$$

It is assumed that in the standard slow-roll approximation, the parameters defined in Eqs. (7) and (8) are small. This kind of assumption, known as the slow-roll approximation, allows for a simplified treatment of the inflationary dynamics. Consequently, the inflationary dynamical equations under such assumptions are simplified, and it leads to:

$$\frac{dN}{d\phi} \simeq -\frac{1}{4VV_{eff,\phi}}. \quad (13)$$

By solving the integral, the scalar field is obtained as a function of the number of e-folds N . Additionally, the Hubble parameter and the quantity χ are expressed in terms of the scalar potential and the GB coupling term as :

$$H^2 \simeq \frac{V(\phi)}{3}, \quad \chi \simeq -4V_{eff,\phi}. \quad (14)$$

By applying the approximations, the slow-roll parameters are expressed in terms of the scalar field. Substituting the solution obtained from Eq. (13) into the slow-roll parameters, the scalar spectral index and the tensor-to-scalar ratio are then derived using Eq. (9), and hence can be expressed as the functions of the number of e-folds N .

After the end of inflation, the decay of the scalar field's energy into standard model particles leads to the repopulation of the universe and the onset of a hot, radiation-dominated era. Since reheating lacks direct observational signatures, it is useful to study this phase indirectly by relating the reheating temperature to inflationary observables [148]. Assuming that the matter content during reheating can be characterized by a constant equation of state parameter ω_{re} , one can derive the following relation [37, 100, 134, 135, 148–151]:

$$N_{re} = \frac{4}{(1 - 3\omega_{re})} \left[61.488 - \ln \left(\frac{V_{end}^{1/4}}{H_k} \right) - N_k \right] \quad (15)$$

$$T_{re} = \left[\left(\frac{43}{11g_{re}} \right)^{1/3} \frac{a_0 T_0}{k} H_k e^{-N_k} \left[\frac{3^2 \cdot 5V_{end}}{\pi^2 g_{re}} \right]^\beta \right]^\gamma, \quad (16)$$

Here, T_{re} and N_{re} denote the reheating temperature and the number of e-folds during reheating, respectively. The quantity N_k represents the number of e-folds from the horizon crossing of a given scale to the end of inflation. The constant parameters β and γ are defined as $\beta = -\frac{1}{3}(1 + \omega_{re})$ and $\gamma = \frac{\beta}{1 - 3\omega_{re}}$, respectively.

IV. CASE I: HYPERBOLIC COUPLING

The consistency of the model with observational data is investigated using slow-roll approximation Eq. (7), (8). These analyses are performed for the two coupling functions introduced in Eq. (11).

As a first case, it is assumed that the GB coupling is described by a *tanh* function, as given in Eq. (11). The analysis begins with the standard slow-roll approximation, which requires solving the integral in Eq. (13). It is assumed that the number of e-folds at horizon crossing is $N_\star = 0$, and that inflation ends at $N = 60$. The initial condition is set at the end of inflation, where the first slow-roll parameter satisfies $\varepsilon_1(\phi_e) = 1$, allowing the determination of the field value at the end of inflation. Solving Eq. (13) yields the scalar field as a function of the number of e-folds during inflation. This solution is then used to compute the slow-roll parameters, the scalar spectral index n_s , and the tensor-to-scalar ratio r as functions of the number of e-folds N .

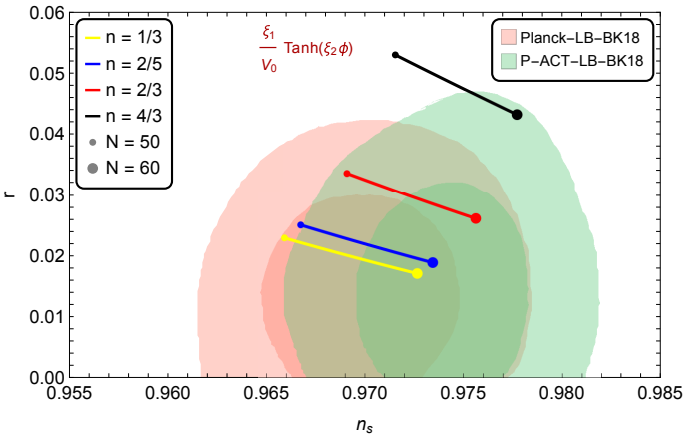


FIG. 1. The plot illustrates the predictions of the model in the $r - n_s$ plane using the standard slow-roll approximation for the case of hyperbolic coupling. The predictions are compared against the ACT observational constraints in the $r - n_s$ plane for various values of the fractional value n , while keeping the coupling fixed at $\xi_1 = 15$, $\xi_2 = 0.255$. Legends are self explanatory.

Figure 1 presents the $r - n_s$ plot obtained from the slow-roll approximation for different values of the power n of the scalar field potential. The larger (smaller) markers correspond to results for $N = 60$ ($N = 50$) e-folds. It is observed that for the values of $n = 1/3$, $2/5$, and setting e-folds to $N = 60$ the prediction lies well within the 1σ of the P-ACT-LB-BK18 constraints. While for $n = 4/3$ for 60 e-folds the results lies in the 2σ region of P-ACT-LB-BK18, but lies outside the *Planck* results, Clearly hints to revisit the cosmology models. We set coupling values to $\xi_1 = 15$ and $\xi_2 = 0.255$, and the the inflation observables n_s and r for all the particular choice of ξ_1 , ξ_2 and n for 50 and 60 e-folds is mentioned in table I. All these results are well within the P-ACT-LB-BK18 dataset, indicating good agreement with ACT observations.

From Fig. 1, it can be seen that increasing the value of n results in rising values of both n_s and r as mentioned in table I. If this trend continues, the predictions eventually fall outside the 2σ bounds of both observational datasets. Similarly, increasing n beyond a certain threshold also pushes the predictions for n_s and r beyond the observationally allowed region. These trends highlight the sensitivity of the model predictions to the choice of the fractional power n of scalar field potential. However, deviations from this optimal value of n or increasing cause the predictions to gradually shift outside the observational bounds of ACT.

Fig. 2 illustrates the parameter space of the free parameters ξ_1 and ξ_2 . For the analysis we scanned the parametric space from 0.001 to 15 for both ξ_1 and ξ_2 . The blue dots represent combinations of (ξ_1, ξ_2) for which the resulting values of n_s and r lie within the 1σ confidence region of the ACT data. The red circular points correspond to values lying in the 2σ region but outside the 1σ bounds. This figure demonstrates the sensitivity of the inflationary predictions to the values of the free parameters. However we can not directly or indirectly put some bound from this analysis on these free parameters of couplings in both the cases (Tanh and Exp).

It is observed that small values of ξ_1 and ξ_2 almost < 1

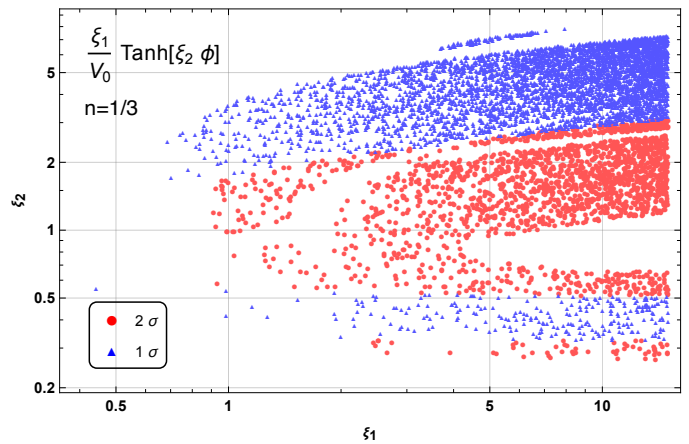


FIG. 2. Hyperbolic Coupling:- The plot shows the allowed region in the $\xi_1 - \xi_2$ parameter space for the case $n = 1/3$. The blue triangular points denote values of (ξ_1, ξ_2) that yield (n_s, r) predictions within the 1σ confidence region of the ACT data. The red circular points correspond to values lying in the 2σ region but outside the 1σ bounds.

are not favored. Within this region and sparse set of (ξ_1, ξ_2) data points satisfies inflationary observables in 1σ or 2σ , contrary for higher values of ξ_1 and ξ_2 significant parametric space satisfies the observational constraints for the said mentioned confidence level of inflationary observables. For consistency with the available inflationary ACT data, this suggests a preference for higher values of non-minimal coupling parameters.

The running of the scalar spectral index given as $\alpha_s = dn_s/d\ln k$, serves as an additional observational constraint for evaluating the viability of an inflationary model. For the parameter values $\xi_1 = 15$, $\xi_2 = 0.255$, the evaluated values of α_s for specific values of n for hyperbolic coupling $\frac{\xi_1}{V_0} \text{Tanh}(\xi_2 \phi)$ are :

$$\begin{cases} n = \frac{1}{3} \Rightarrow \alpha_s = -0.000546025, \\ n = \frac{2}{5} \Rightarrow \alpha_s = -0.000552645, \\ n = \frac{2}{3} \Rightarrow \alpha_s = -0.000534904, \\ n = \frac{4}{3} \Rightarrow \alpha_s = -0.000499958. \end{cases}$$

Notably for high regime of one of the ξ , favors the n_s and r results within the observational constraints. The results for α_s still lie inside the bounds imposed by latest ACT observations.

After the end of inflation, the Universe undergoes a reheating phase that ensures a smooth transition to the radiation era. In Fig. 3 we have shown the behavior of N_{re} and T_{re} with the spectral index n_s . To obtain this plot we have used Eqs. (15) and (16), where the free parameters of hyperbolic coupling are chosen to be $\xi_1 = 15$ and $\xi_2 = 0.255$.

The top panel illustrates the influence of N_{re} on the scalar spectral index (n_s) . As shown in Fig. 1, for the above mentioned values of ξ_1 and ξ_2 , parameters, the scalar spectral index is found to be $n_s \simeq 0.9726$ for $N_k = 60$ and for power of potential $n = 1/3$. This value of n_s corresponds to reheating e-fold numbers $N_{re} \simeq 11.57$ and 5.78 for $\omega_{re} = 2/3$ and 1, respectively. The bottom panel is the variation of

Coupling Type	N	$n = \frac{1}{3}$		$n = \frac{2}{5}$		$n = \frac{2}{3}$		$n = \frac{4}{3}$	
		n_s	r	n_s	r	n_s	r	n_s	r
$\frac{\xi_1}{V_0} \tanh(\xi_2 \phi)$	50	0.96592	0.02290	0.96674	0.02503	0.96910	0.03353	0.97155	0.05300
	60	0.97265	0.01707	0.97344	0.01885	0.97562	0.02610	0.97772	0.04319
$\frac{\xi_1}{V_0} \exp(-\xi_2 \phi)$	50	0.97329	0.02011	0.97228	0.02368	0.96693	0.03373	0.92793	0.01333
	60	0.97738	0.01618	0.97648	0.01897	0.97155	0.02615	0.93218	0.00699

TABLE I. Comparison of n_s and r for different values of fractional potential power n and at different e-fold N under two different coupling types: Tanh hyperbolic and Exponential.

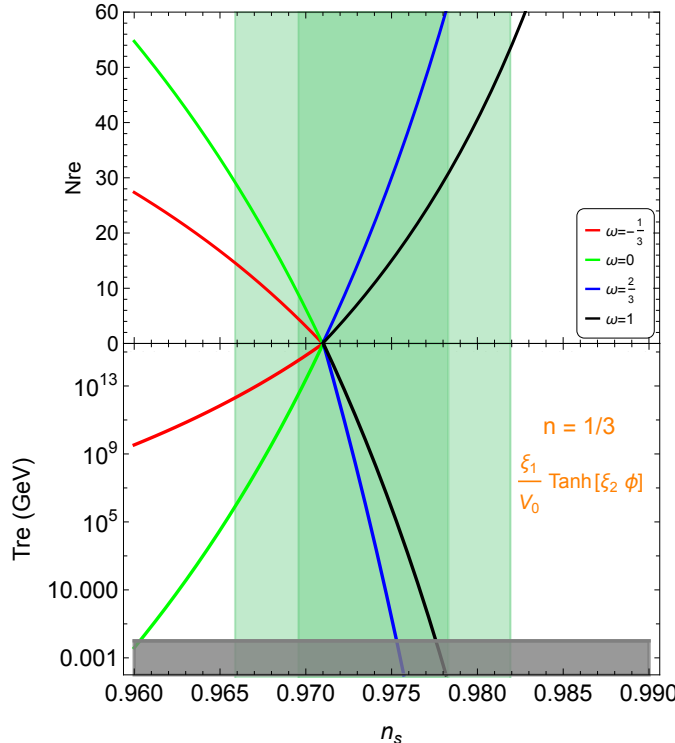


FIG. 3. The plot shows the relation of n_s with the reheating phase, so that the top panel shows the behavior of the reheating e-fold N_{re} versus n_s , and the bottom panel describes the behavior of the reheating temperature T_{re} versus n_s . The result provided for different choice of the reheating equation of state ω_{re} , as $\omega_{re} = -1/3$ (red-curve), $\omega_{re} = 0$ (green-curve), $\omega_{re} = 2/3$ (blue-curve), $\omega_{re} = 1$ (black-curve). The gray area at the bottom is the excluded region originating from the BBN constraint.

the reheating temperature as a function of the scalar spectral index. It is observed that higher values of the reheating equation-of-state parameter ω_{re} correspond to smaller reheating e-folds N_{re} , which in turn result in higher reheating temperatures. For example, for $\omega_{re} = 2/3$ and 1, the reheating temperature is found to be $T_{re} \simeq 2.33 \times 10^9$ GeV and 6.62×10^{11} GeV, respectively. It is crucial to emphasize that the obtained reheating temperature must comply with both the constraints from ACT data and the lower bound set by Big Bang Nucleosynthesis (BBN), $T_{re} \gtrsim 10$ MeV.

V. CASE II: EXPONENTIAL COUPLING

In case II, the consistency of this model is tested with the observational data investigated using the standard slow-roll approximations taking in consideration the second GB coupling as mention in Eq.(11). In fig. 4 the yellow, blue, red lines represents the n_s and r dynamics while going from 50 to 60 e-folds, with $n = 1/3, 2/5$ and $2/3$ values of the fractional power n respectively and the values for $n = 4/3$ lies outside of this $r - n_s$ plane.¹ It is observed that increasing n leads to a shift towards the lower side of scalar spectral index n_s and substantial increase in the tensor-to-scalar ratio r . For $\xi_1 = 0.5$ and $\xi_2 = 0.01$, for $n = 1/3$ and $2/5$ the values of n_s and r lie in the 1σ contour of P-ACT-LB-BK18 dataset. However, as the value of n increases eventually the n_s and r points move out 1σ region. Even for the mentioned free coupling parameters, for $n = 2/3$ and $N = 50$ the inflationary observables lie outside the of P-ACT-LB-BK18 contour. The $r - n_s$ trajectories derived from the slow-roll approximation in Fig.(5) are subjected to change on changing free coupling parameters ξ_1 and ξ_2 .

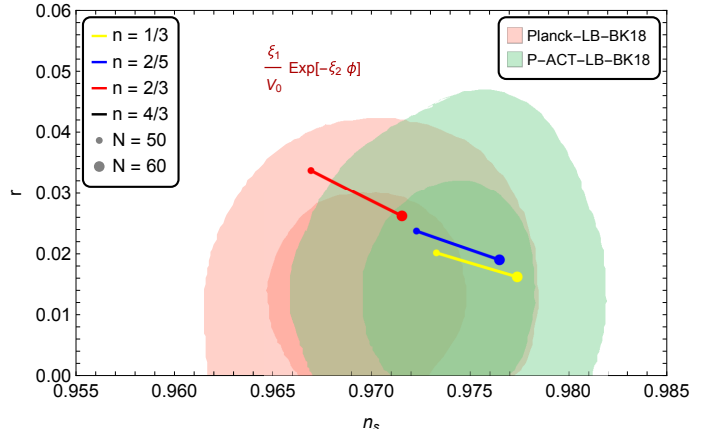


FIG. 4. The plot illustrates the predictions of the model in the $r - n_s$ plane using the standard slow-roll approximation for the case of exponential coupling. The predictions are compared against the ACT observational constraints in the $r - n_s$ plot for various values of the fractional value n , while keeping the coupling fixed at $\xi_1 = 0.5$, $\xi_2 = 0.01$. Legends are self explanatory.

¹ For $n = 4/3$ the data points lies outside the $n_s - r$ plane. For $N = 50$ $n_s = 0.92793$ and $r = 0.01333$ and for $N = 60$ $n_s = 0.93218$ and $r = 0.00699$.

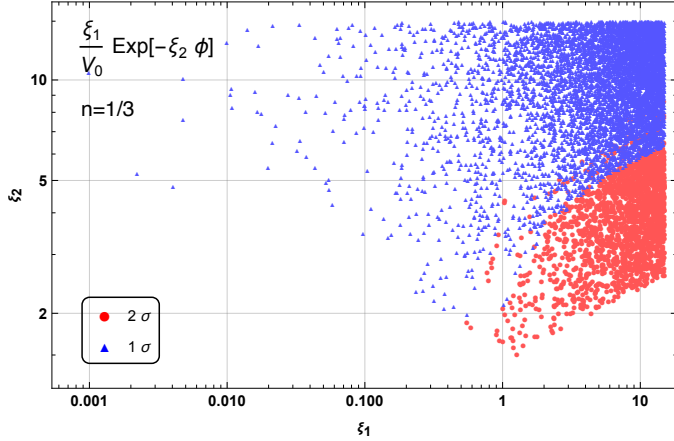


FIG. 5. Exponential Coupling:- The plot shows the allowed region in the ξ_1 - ξ_2 parameter space for the case $n = 1/3$. The blue triangular points denote values of (ξ_1, ξ_2) that yield (n_s, r) predictions within the 1σ confidence region of the ACT data. The red circular points correspond to values lying in the 2σ region but outside the 1σ bounds.

The analysis for Fig.5 is carried out in a same way as for Fig.2 for the same values of ξ_1 and ξ_2 from 0.001 to 15. In this plot, blue dots represent the combinations of (ξ_1, ξ_2) for which the predicted values of n_s and r lie within the 1σ confidence level. The red points corresponds to the parameter sets (n_s, r) those which are consistent with the broader 2σ region but outside the 1σ region. The allowed interval for ξ_2 depends sensitively on the choice of ξ_1 . For instance, when $\xi_1 = 10$, the model remains compatible with the 1σ region of ACT observations provided $5 < \xi_2 \leq 15$. This permissible range of ξ_2 expands with increase in ξ_1 value. However the narrow ξ -regime is least favored to satisfy inflationary observables. The density of points in both 1σ and 2σ is more and favors higher values of free coupling parameters. But for 1σ the permissible range of ξ_2 narrows on both side around the $\xi_1 = 1$. For example, at $\xi_1 = 1$, the valid range expands to $2 < \xi_2 < 15$, but for $\xi_1 = 10$, the valid range expands to $5.5 < \xi_2 \leq 15$. Similar trend is followed for 2σ region.

Taking into account the running of the scalar spectral index, it is found that for $\xi_1 = 0.5$, $\xi_2 = 0.01$, the evaluated values of α_s for the exponential coupling $\frac{\xi_1}{V_0} \exp(-\xi_2 \phi)$ are:

$$\begin{cases} n = \frac{1}{3} \Rightarrow \alpha_s = -0.000341584, \\ n = \frac{2}{5} \Rightarrow \alpha_s = -0.000350776, \\ n = \frac{2}{3} \Rightarrow \alpha_s = -0.000386625, \\ n = \frac{4}{3} \Rightarrow \alpha_s = -0.000339927. \end{cases}$$

The results for running of the scalar spectral index we show here are compatible with the recent ACT observations.

The results of the reheating phase analysis are presented in Fig. 6, which illustrates the influence of the reheating e-fold number and reheating temperature on the scalar spectral index. The plot shows how both N_{re} and T_{re} vary with n_s for different values of the reheating equation-of-state parameter ω_{re} , with the free parameters fixed at $\xi_1 = 0.5$ and $\xi_2 = 0.01$ and for fractional power $n = 1/3$. As inferred from Fig. 4, for these parameter choices, the scalar spectral

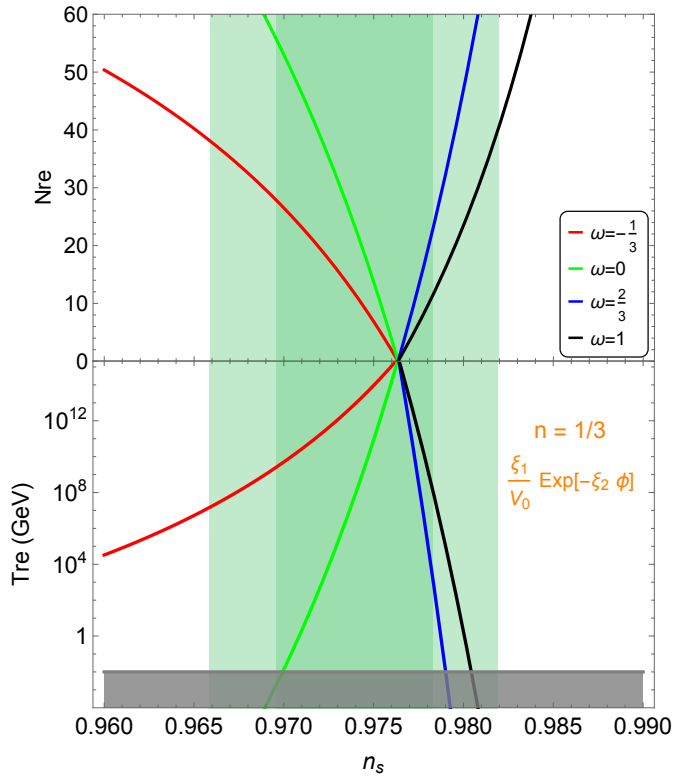


FIG. 6. The relation of n_s with the reheating number of e-folds N_{re} is shown in the top panel, and the bottom panel displays the relation between n_s and the reheating temperature T_{re} . The plot includes the results for different values of the reheating equation of state parameter as: $\omega_{re} = -1/3$ (red-curve), $\omega_{re} = 0$ (green-curve), $\omega_{re} = 2/3$ (blue-curve), $\omega_{re} = 1$ (black-curve). The grey area at the bottom is the excluded region originating from the BBN constraint.

index for $N_k = 60$ is approximately $n_s = 0.97738$ lies in 2σ region. This value corresponds to $N_{re} \simeq 11.51$ and 5.75 for $\omega_{re} = 2/3$ and 1, respectively. As ω_{re} increases, the reheating e-fold decreases, leading to a higher reheating temperature, as depicted in the bottom panel. The resulting reheating temperatures are roughly $T_{re} \simeq 2.39 \times 10^9$ GeV and 6.62×10^{11} GeV for the respective values of ω_{re} .

VI. CONCLUSION

The latest observational results from the ACT collaboration suggest a higher scalar spectral index, reported as $n_s = 0.9743 \pm 0.0034$, which is notably larger than the earlier estimate from the Planck mission [12]. This upward shift in n_s poses a significant challenge to many inflationary models that were previously consistent with Planck data. As a result, several inflationary models, are now disfavored under the new ACT observations.

In this work, we investigated inflationary dynamics within the framework of EGB gravity, incorporating a fractional scalar potential. The EGB theory introduces a quadratic curvature correction to the standard Einstein–Hilbert action through a non-minimal coupling between the scalar field and the Gauss–Bonnet term. We analyzed two distinct forms of the coupling function, namely

$\xi(\phi) \propto \tanh(\xi_2\phi)$ and $\xi(\phi) \propto \exp(\xi_2\phi)$. Owing to the modified field equations arising from the Gauss–Bonnet interaction, the model offers a viable framework for accommodating inflationary potentials for the different values of n that are otherwise ruled out by the latest observational constraints from ACT.

We employed the slow-roll approximation to evaluate the model’s predictions for the scalar spectral index n_s and the tensor-to-scalar ratio r . The resulting $r-n_s$ values were compared with observational bounds by plotting them on the $r-n_s$ plane for the different fractional values of n of the scalar potential, constrained by ACT data. The calculated values of n_s and r (for numerical values, see Table. I) fall within the 1σ confidence region of the ACT observations, indicating good agreement between the theoretical model and data.

To further analyze the model, we explore the parameter space of the coupling coefficients ξ_1 and ξ_2 . For the case of tanh-type coupling, it was observed that higher values of ξ_1 and ξ_2 results in the better agreement with the bounds imposed on the $r - n_s$ by the ACT observations (see Fig. 2). A similar trend can be seen for the other coupling function (Exp). Where higher values of ξ_1 and ξ_2 results in observationally viable values of $r - n_s$ (see Fig. 5). Finally, we examined the running of the scalar spectral index (α_s) for both type of coupling function mentioned in Eq. (11)

and the results remains consistent with the observational bounds.

At the final stage of our analysis, we examined the reheating phase by plotting the variation of the reheating e-fold number N_{re} and the reheating temperature T_{re} with respect to the scalar spectral index n_s . The results indicated that, in order to simultaneously satisfy the ACT observational constraint $n_s = 0.974$ and the bounds on the reheating temperature, the equation-of-state parameter during reheating must lie in the range $\omega_{\text{re}} > 1/3$. Furthermore, it was observed that increasing ω_{re} leads to a decrease in the number of reheating e-folds and an increase in the reheating temperature.

In our future work, we aim to investigate the formation of Primordial Black Holes (PBHs) and the generation of Scalar-Induced Gravitational Waves (SIGWs) within the context of modified gravity theories [133, 136, 152, 153].

ACKNOWLEDGEMENTS

The authors thank Yogesh for discussing the idea for this project and his continued suggestions and insightful discussions throughout its development.

-
- [1] A. H. Guth, *Phys. Rev. D* **23**, 347 (1981).
 - [2] A. D. Linde, *Phys. Lett. B* **108**, 389 (1982).
 - [3] V. F. Mukhanov and G. V. Chibisov, *JETP Lett.* **33**, 532 (1981).
 - [4] K. Sato, *Mon. Not. Roy. Astron. Soc.* **195**, 467 (1981).
 - [5] A. A. Starobinsky, in *30 Years of the Landau Institute*, Vol. 11, edited by I. M. Khalatnikov and V. P. Mineev (1996) p. 771.
 - [6] A. Albrecht and P. J. Steinhardt, *Phys. Rev. Lett.* **48**, 1220 (1982).
 - [7] A. A. Starobinsky, *Phys. Lett. B* **91**, 99 (1980).
 - [8] A. A. Starobinsky, *Phys. Lett. B* **117**, 175 (1982).
 - [9] A. A. Starobinsky, *Sov. Astron. Lett.* **9**, 302 (1983).
 - [10] G. Hinshaw *et al.* (WMAP), *Astrophys. J. Suppl.* **208**, 19 (2013), arXiv:1212.5226 [astro-ph.CO].
 - [11] P. A. R. Ade *et al.* (Planck), *Astron. Astrophys.* **594**, A20 (2016), arXiv:1502.02114 [astro-ph.CO].
 - [12] Y. Akrami *et al.* (Planck), *Astron. Astrophys.* **641**, A10 (2020), arXiv:1807.06211 [astro-ph.CO].
 - [13] G. Barenboim and W. H. Kinney, *JCAP* **0703**, 014 (2007), arXiv:astro-ph/0701343 [astro-ph].
 - [14] P. Franche, R. Gwyn, B. Underwood, and A. Wissanji, *Phys. Rev. D* **82**, 063528 (2010), arXiv:1002.2639 [hep-th].
 - [15] S. Unnikrishnan, V. Sahni, and A. Toporensky, *JCAP* **1208**, 018 (2012), arXiv:1205.0786 [astro-ph.CO].
 - [16] K. Saaidi, A. Mohammadi, and T. Golanbari, *Adv. High Energy Phys.* **2015**, 926807 (2015), arXiv:1708.03675 [gr-qc].
 - [17] A. Mohammadi, Z. Ossoulian, T. Golanbari, and K. Saaidi, *Astrophys. Space Sci.* **359**, 7 (2015).
 - [18] M. Fairbairn and M. H. G. Tytgat, *Phys. Lett. B* **546**, 1 (2002), arXiv:hep-th/0204070 [hep-th].
 - [19] A. Aghamohammadi, A. Mohammadi, T. Golanbari, and K. Saaidi, *Phys. Rev. D* **90**, 084028 (2014), arXiv:1502.07578 [gr-qc].
 - [20] D. Bessada, W. H. Kinney, and K. Tzirakis, *JCAP* **0909**, 031 (2009), arXiv:0907.1311 [gr-qc].
 - [21] J. M. Weller, C. van de Bruck, and D. F. Mota, *JCAP* **1206**, 002 (2012), arXiv:1111.0237 [astro-ph.CO].
 - [22] N. Nazavari, A. Mohammadi, Z. Ossoulian, and K. Saaidi, *Phys. Rev. D* **93**, 123504 (2016), arXiv:1708.03676 [gr-qc].
 - [23] R. Amani, K. Rezazadeh, A. Abdolmaleki, and K. Karami, *Astrophys. J.* **853**, 188 (2018), arXiv:1802.06075 [astro-ph.CO].
 - [24] T. Golanbari, A. Mohammadi, and K. Saaidi, *Phys. Dark Univ.* **27**, 100456 (2020), arXiv:1808.07246 [gr-qc].
 - [25] A. Berera, *Physical Review Letters* **75**, 3218 (1995).
 - [26] A. Berera, *Nuclear Physics B* **585**, 666 (2000).
 - [27] M. Bastero-Gil and A. Berera, *Phys. Rev. D* **71**, 063515 (2005), arXiv:hep-ph/0411144 [hep-ph].
 - [28] K. Sayar, A. Mohammadi, L. Akhtari, and K. Saaidi, *Phys. Rev. D* **95**, 023501 (2017), arXiv:1708.01714 [gr-qc].
 - [29] L. Akhtari, A. Mohammadi, K. Sayar, and K. Saaidi, *Astropart. Phys.* **90**, 28 (2017), arXiv:1710.05793 [astro-ph.CO].
 - [30] H. Sheikhamadi, A. Mohammadi, A. Aghamohammadi, T. Harko, R. Herrera, C. Corda, A. Abebe, and K. Saaidi, *Eur. Phys. J. C* **79**, 1038 (2019), arXiv:1907.10966 [gr-qc].
 - [31] H. Motohashi, A. A. Starobinsky, and J. Yokoyama, *JCAP* **1509**, 018 (2015), arXiv:1411.5021 [astro-ph.CO].
 - [32] S. D. Odintsov, V. K. Oikonomou, and L. Sebastiani, *Nucl. Phys. B* **923**, 608 (2017), arXiv:1708.08346 [gr-qc].
 - [33] V. K. Oikonomou, *Mod. Phys. Lett. A* **32**, 1750172 (2017), arXiv:1706.00507 [gr-qc].
 - [34] A. Mohammadi, T. Golanbari, and K. Saaidi, *Phys. Dark Univ.* **28**, 100505 (2020), arXiv:1912.07006 [gr-qc].
 - [35] A. Mohammadi, T. Golanbari, S. Nasri, and K. Saaidi, *Phys. Rev. D* **101**, 123537 (2020), arXiv:2004.12137 [gr-qc].

- [36] A. Mohammadi, *Phys. Dark Univ.* **36**, 101055 (2022), arXiv:2203.06643 [gr-qc].
- [37] R. Adhikari, M. R. Gangopadhyay, and Yogesh, *Eur. Phys. J. C* **80**, 899 (2020), arXiv:2002.07061 [astro-ph.CO].
- [38] A. Mohammadi and F. Kheirandish, *Phys. Dark Univ.* **42**, 101362 (2023).
- [39] T. Louis *et al.* (ACT), arXiv preprint (2025), arXiv:2503.14452 [astro-ph.CO].
- [40] E. Calabrese *et al.* (ACT), arXiv preprint (2025), arXiv:2503.14454 [astro-ph.CO].
- [41] R. Kallosh, A. Linde, and D. Roest, (2025), arXiv:2503.21030 [hep-th].
- [42] S. Aoki, H. Otsuka, and R. Yanagita, (2025), arXiv:2504.01622 [hep-ph].
- [43] C. Dioguardi, A. J. Iovino, and A. Racioppi, *Phys. Lett. B* **868**, 139664 (2025), arXiv:2504.02809 [gr-qc].
- [44] A. Salvio, (2025), arXiv:2504.10488 [hep-ph].
- [45] S. Brahma and J. Calderón-Figueroa, (2025), arXiv:2504.02746 [astro-ph.CO].
- [46] Q. Gao, Y. Gong, Z. Yi, and F. Zhang, (2025), arXiv:2504.15218 [astro-ph.CO].
- [47] M. Drees and Y. Xu, (2025), arXiv:2504.20757 [astro-ph.CO].
- [48] D. S. Zharov, O. O. Sobol, and S. I. Vilchinskii, (2025), arXiv:2505.01129 [astro-ph.CO].
- [49] W. Yin, (2025), arXiv:2505.03004 [hep-ph].
- [50] L. Liu, Z. Yi, and Y. Gong, (2025), arXiv:2505.02407 [astro-ph.CO].
- [51] I. D. Gialamas, T. Katsoulas, and K. Tamvakis, (2025), arXiv:2505.03608 [gr-qc].
- [52] M. R. Haque, S. Pal, and D. Paul, (2025), arXiv:2505.01517 [astro-ph.CO].
- [53] M. R. Haque, S. Pal, and D. Paul, (2025), arXiv:2505.04615 [astro-ph.CO].
- [54] C. Dioguardi and A. Karam, (2025), arXiv:2504.12937 [gr-qc].
- [55] I. D. Gialamas, A. Karam, A. Racioppi, and M. Raidal, (2025), arXiv:2504.06002 [astro-ph.CO].
- [56] Yogesh, A. Mohammadi, Q. Wu, and T. Zhu, (2025), arXiv:2505.05363 [astro-ph.CO].
- [57] A. Mohammadi, Yogesh, and A. Wang, (2025), arXiv:2507.06544 [astro-ph.CO].
- [58] N. S. Risdianto, R. H. S. Budhi, N. Shobcha, and A. S. Adam, (2025), arXiv:2507.12868 [gr-qc].
- [59] E. G. Ferreira, E. McDonough, L. Balkenhol, R. Kallosh, and L. Knox, (2025), arXiv:2507.12459 [astro-ph.CO].
- [60] A. Mohammadi, Yogesh, and A. Wang, (2025), arXiv:2507.06544 [astro-ph.CO].
- [61] C. Pallis, (2025), arXiv:2507.02219 [hep-ph].
- [62] Q. Gao, Y. Qian, Y. Gong, and Z. Yi, (2025), arXiv:2506.18456 [gr-qc].
- [63] N. Okada and O. Seto, (2025), arXiv:2506.15965 [hep-ph].
- [64] J. McDonald, (2025), arXiv:2506.12916 [hep-ph].
- [65] E. Bianchi and M. Gamonal, (2025), arXiv:2506.10081 [gr-qc].
- [66] S. Odintsov and V. Oikonomou, (2025), arXiv:2506.08193 [gr-qc].
- [67] K. Kohri and X. Wang, (2025), arXiv:2506.06797 [astro-ph.CO].
- [68] A. Chakraborty, D. Maity, and R. Mondal, (2025), arXiv:2506.02141 [astro-ph.CO].
- [69] C. Pallis, (2025), arXiv:2505.23243 [hep-ph].
- [70] D. Frolovsky and S. V. Ketov, (2025), arXiv:2505.17514 [astro-ph.CO].
- [71] M. R. Haque and D. maity, (2025), arXiv:2505.18267 [astro-ph.CO].
- [72] Z.-Z. Peng, Z.-C. Chen, and L. Liu, (2025), arXiv:2505.12816 [astro-ph.CO].
- [73] R. C. Bernardo, S. Koh, and G. Tumurtushaa, (2025), arXiv:2505.10235 [astro-ph.CO].
- [74] Z. Yi, X. Wang, Q. Gao, and Y. Gong, (2025), arXiv:2505.10268 [astro-ph.CO].
- [75] A. Addazi, Y. Aldabergenov, and S. V. Ketov, (2025), arXiv:2505.10305 [gr-qc].
- [76] S. Maity, (2025), arXiv:2505.10534 [astro-ph.CO].
- [77] C. T. Byrnes, M. Cortés, and A. R. Liddle, (2025), arXiv:2505.09682 [astro-ph.CO].
- [78] D. Zharov, O. Sobol, and S. Vilchinskii, (2025), arXiv:2505.01129 [astro-ph.CO].
- [79] L. Kofman, A. D. Linde, and A. A. Starobinsky, *Phys. Rev. Lett.* **73**, 3195 (1994), arXiv:hep-th/9405187.
- [80] K. D. Lozanov, (2019), arXiv:1907.04402 [astro-ph.CO].
- [81] L. Kofman, in *3rd RESCEU International Symposium on Particle Cosmology* (1997) pp. 1–8, arXiv:hep-ph/9802285.
- [82] F. L. Bezrukov and M. Shaposhnikov, *Phys. Lett. B* **659**, 703 (2008), arXiv:0710.3755 [hep-th].
- [83] F. Bezrukov, A. Magnin, M. Shaposhnikov, and S. Sibiryakov, *JHEP* **01**, 016 (2011), arXiv:1008.5157 [hep-ph].
- [84] A. O. Barvinsky and A. Y. Kamenshchik, *Phys. Lett. B* **332**, 270 (1994), arXiv:gr-qc/9404062.
- [85] J. L. Cervantes-Cota and H. Dehnen, *Nucl. Phys. B* **442**, 391 (1995), arXiv:astro-ph/9505069.
- [86] A. O. Barvinsky, A. Y. Kamenshchik, and A. A. Starobinsky, *JCAP* **11**, 021 (2008), arXiv:0809.2104 [hep-ph].
- [87] A. De Simone, M. P. Hertzberg, and F. Wilczek, *Phys. Lett. B* **678**, 1 (2009), arXiv:0812.4946 [hep-ph].
- [88] I. D. Gialamas, A. Karam, A. Lykkas, and T. D. Pappas, *Phys. Rev. D* **102**, 063522 (2020), arXiv:2008.06371 [gr-qc].
- [89] F. L. Bezrukov, A. Magnin, and M. Shaposhnikov, *Phys. Lett. B* **675**, 88 (2009), arXiv:0812.4950 [hep-ph].
- [90] R. Kallosh and A. Linde, *JCAP* **06**, 027 (2013), arXiv:1306.3211 [hep-th].
- [91] A. O. Barvinsky, A. Y. Kamenshchik, C. Kiefer, A. A. Starobinsky, and C. F. Steinwachs, *Eur. Phys. J. C* **72**, 2219 (2012), arXiv:0910.1041 [hep-ph].
- [92] J. Rubio, *Front. Astron. Space Sci.* **5**, 50 (2019), arXiv:1807.02376 [hep-ph].
- [93] I. D. Gialamas, A. Karam, T. D. Pappas, and E. Tomberg, *Int. J. Geom. Meth. Mod. Phys.* **20**, 2330007 (2023), arXiv:2303.14148 [gr-qc].
- [94] I. D. Gialamas and K. Tamvakis, *JCAP* **03**, 042 (2023), arXiv:2212.09896 [gr-qc].
- [95] I. D. Gialamas, A. Karam, T. D. Pappas, and V. C. Spanos, *Phys. Rev. D* **104**, 023521 (2021), arXiv:2104.04550 [astro-ph.CO].
- [96] I. D. Gialamas, A. Karam, and A. Racioppi, *JCAP* **11**, 014 (2020), arXiv:2006.09124 [gr-qc].
- [97] J. Kim, Z. Yang, and Y.-l. Zhang, (2025), arXiv:2503.16907 [astro-ph.CO].
- [98] J. Kim, X. Wang, Y.-l. Zhang, and Z. Ren, (2025), arXiv:2504.12035 [astro-ph.CO].
- [99] Yogesh, I. A. Bhat, and M. R. Gangopadhyay, (2024), arXiv:2408.01670 [astro-ph.CO].
- [100] Yogesh and M. R. Gangopadhyay, *JHEAp* **44**, 214 (2024).
- [101] A. S. Koshelev, K. S. Kumar, and A. A. Starobinsky, *Int. J. Mod. Phys. D* **29**, 2043018 (2020), arXiv:2005.09550 [hep-th].
- [102] C. van de Bruck and C. Longden, *Phys. Rev. D* **93**, 063519 (2016), arXiv:1512.04768 [hep-ph].

- [103] Z.-K. Guo and D. J. Schwarz, *Phys. Rev. D* **80**, 063523 (2009), arXiv:0907.0427 [hep-th].
- [104] S. Koh, B.-H. Lee, and G. Tumurtushaa, *Phys. Rev. D* **95**, 123509 (2017), arXiv:1610.04360 [gr-qc].
- [105] M. Satoh and J. Soda, *JCAP* **09**, 019 (2008), arXiv:0806.4594 [astro-ph].
- [106] P.-X. Jiang, J.-W. Hu, and Z.-K. Guo, *Phys. Rev. D* **88**, 123508 (2013), arXiv:1310.5579 [hep-th].
- [107] S. Koh, B.-H. Lee, and G. Tumurtushaa, *Phys. Rev. D* **98**, 103511 (2018), arXiv:1807.04424 [astro-ph.CO].
- [108] J. Mathew and S. Shankaranarayanan, *Astropart. Phys.* **84**, 1 (2016), arXiv:1602.00411 [astro-ph.CO].
- [109] E. O. Pozdeeva, M. R. Gangopadhyay, M. Sami, A. V. Toporensky, and S. Y. Vernov, *Phys. Rev. D* **102**, 043525 (2020), arXiv:2006.08027 [gr-qc].
- [110] E. O. Pozdeeva, M. A. Skugoreva, A. V. Toporensky, and S. Y. Vernov, *JCAP* **12**, 006 (2016), arXiv:1608.08214 [gr-qc].
- [111] K. Nozari and N. Rashidi, *Phys. Rev. D* **95**, 123518 (2017), arXiv:1705.02617 [astro-ph.CO].
- [112] S. D. Odintsov and V. K. Oikonomou, *Phys. Rev. D* **98**, 044039 (2018), arXiv:1808.05045 [gr-qc].
- [113] I. V. Fomin and S. V. Chervon, *Phys. Rev. D* **100**, 023511 (2019), arXiv:1903.03974 [gr-qc].
- [114] S. D. Odintsov, V. K. Oikonomou, and F. P. Fronimos, *Nucl. Phys. B* **958**, 115135 (2020), arXiv:2003.13724 [gr-qc].
- [115] S. D. Odintsov and V. K. Oikonomou, *Phys. Lett. B* **805**, 135437 (2020), arXiv:2004.00479 [gr-qc].
- [116] S. Kawai and J. Kim, *Phys. Rev. D* **104**, 043525 (2021), arXiv:2105.04386 [hep-ph].
- [117] S. Kawai and J. Kim, *Phys. Lett. B* **789**, 145 (2019), arXiv:1702.07689 [hep-th].
- [118] V. K. Oikonomou, *Astropart. Phys.* **141**, 102718 (2022), arXiv:2204.06304 [gr-qc].
- [119] V. K. Oikonomou, P. D. Katzianis, and I. C. Papadimitriou, *Class. Quant. Grav.* **39**, 095008 (2022), arXiv:2203.09867 [gr-qc].
- [120] G. Cognola, E. Elizalde, S. Nojiri, S. Odintsov, and S. Zerbini, *Phys. Rev. D* **75**, 086002 (2007), arXiv:hep-th/0611198.
- [121] S. D. Odintsov, V. K. Oikonomou, and F. P. Fronimos, *Annals Phys.* **420**, 168250 (2020), arXiv:2007.02309 [gr-qc].
- [122] S. Nojiri, S. D. Odintsov, V. K. Oikonomou, N. Chatzarakis, and T. Paul, *Eur. Phys. J. C* **79**, 565 (2019), arXiv:1907.00403 [gr-qc].
- [123] V. K. Oikonomou, *Phys. Lett. B* **856**, 138890 (2024), arXiv:2407.12155 [gr-qc].
- [124] V. K. Oikonomou, P. Tsypba, and O. Razina, *Annals Phys.* **462**, 169597 (2024), arXiv:2401.11273 [gr-qc].
- [125] S. D. Odintsov, V. K. Oikonomou, I. Giannakoudi, F. P. Fronimos, and E. C. Lymperiadou, *Symmetry* **15**, 1701 (2023), arXiv:2307.16308 [gr-qc].
- [126] S. Kawai, M.-a. Sakagami, and J. Soda, *Phys. Lett. B* **437**, 284 (1998), arXiv:gr-qc/9802033.
- [127] S. Nojiri and S. D. Odintsov, (2024), arXiv:2406.12558 [gr-qc].
- [128] E. Elizalde, S. Nojiri, S. D. Odintsov, and V. K. Oikonomou, *Phys. Dark Univ.* **45**, 101536 (2024), arXiv:2312.02889 [gr-qc].
- [129] S. Nojiri, S. D. Odintsov, and D. Sáez-Chillón Gómez, *Phys. Dark Univ.* **41**, 101238 (2023), arXiv:2304.08255 [gr-qc].
- [130] S. D. Odintsov, V. K. Oikonomou, and F. P. Fronimos, *Phys. Rev. D* **107**, 08 (2023), arXiv:2303.14594 [gr-qc].
- [131] S. D. Odintsov and V. K. Oikonomou, *Phys. Lett. B* **833**, 137353 (2022), arXiv:2206.06024 [gr-qc].
- [132] S. Kawai and J. Kim, *Phys. Rev. D* **108**, 103537 (2023), arXiv:2308.13272 [astro-ph.CO].
- [133] Yogesh and A. Mohammadi, *Astrophys. J.* **986**, 35 (2025), arXiv:2501.01867 [gr-qc].
- [134] H. A. Khan and Yogesh, *Phys. Rev. D* **105**, 063526 (2022), arXiv:2201.06439 [astro-ph.CO].
- [135] M. R. Gangopadhyay, H. A. Khan, and Yogesh, *Phys. Dark Univ.* **40**, 101177 (2023), arXiv:2205.15261 [astro-ph.CO].
- [136] S. Kawai and J. Kim, *Phys. Rev. D* **104**, 083545 (2021), arXiv:2108.01340 [astro-ph.CO].
- [137] A. Ashrafpour and K. Karami, *Astrophys. J.* **965**, 11 (2024), arXiv:2309.16356 [astro-ph.CO].
- [138] Yogesh, M. Zahoor, K. A. Wani, and I. A. Bhat, *Phys. Dark Univ.* **47**, 101732 (2025), arXiv:2505.11429 [astro-ph.CO].
- [139] E. O. Pozdeeva, *Eur. Phys. J. C* **80**, 612 (2020), arXiv:2005.10133 [gr-qc].
- [140] Z. Yi, Y. Gong, and M. Sabir, *Phys. Rev. D* **98**, 083521 (2018), arXiv:1804.09116 [gr-qc].
- [141] K. Kleidis and V. K. Oikonomou, *Nucl. Phys. B* **948**, 114765 (2019), arXiv:1909.05318 [gr-qc].
- [142] N. Rashidi and K. Nozari, *Astrophys. J.* **890**, 58 (2020), arXiv:2001.07012 [astro-ph.CO].
- [143] E. O. Pozdeeva, M. A. Skugoreva, A. V. Toporensky, and S. Y. Vernov, *JCAP* **09**, 050 (2024), arXiv:2403.06147 [gr-qc].
- [144] K. Harigaya, M. Ibe, K. Schmitz, and T. T. Yanagida, *Physical Review D* **90** (2014), 10.1103/physrevd.90.123524.
- [145] A. Ashrafpour and K. Karami, *The Astrophysical Journal* **965**, 11 (2024).
- [146] E. O. Pozdeeva, M. Sami, A. V. Toporensky, and S. Y. Vernov, *Phys. Rev. D* **100**, 083527 (2019), arXiv:1905.05085 [gr-qc].
- [147] S. Vernov and E. Pozdeeva, *Universe* **7**, 149 (2021), arXiv:2104.11111 [gr-qc].
- [148] J. L. Cook, E. Dimastrogiovanni, D. A. Easson, and L. M. Krauss, *JCAP* **04**, 047 (2015), arXiv:1502.04673 [astro-ph.CO].
- [149] R. Adhikari, M. R. Gangopadhyay, and Yogesh, *Grav. Cosmol.* **28**, 1 (2022), arXiv:1909.07217 [astro-ph.CO].
- [150] I. D. Gialamas and A. B. Lahanas, *Phys. Rev. D* **101**, 084007 (2020), arXiv:1911.11513 [gr-qc].
- [151] Yogesh, M. R. Gangopadhyay, and A. Wang, (2024), arXiv:2408.00316 [gr-qc].
- [152] M. R. Gangopadhyay, V. V. Godithi, R. Inui, K. Ichiki, T. Kajino, A. Manusankar, G. J. Mathews, and Yogesh, *JHEAp* **47**, 100358 (2025), arXiv:2309.03101 [astro-ph.CO].
- [153] M. R. Gangopadhyay, J. C. Jain, D. Sharma, and Yogesh, *Eur. Phys. J. C* **82**, 849 (2022), arXiv:2108.13839 [astro-ph.CO].